SLENDER HIGH-STRENGTH CONCRETE COLUMNS SUBJECTED TO ECCENTRIC LOADING

By Christina Claeson[1] and Kent Gylltoft[2]

ABSTRACT: An experimental study of the behavior of reinforced concrete columns and results of a nonlinear finite-element analysis are presented. Twelve full-scale columns with square sections were tested under eccentric monotonic loading. Effects of key parameters such as concrete strength, stirrup spacing, slenderness of the columns, and eccentricity of the applied axial load were studied. Significant gains in load capacity were obtained with increased concrete strength. The results of the finite-element analysis correlate well with the results of the tests. A parametric study was made to examine the difference in failure modes for the different concrete strengths, length-to-width ratios, and loading eccentricities. The higher compressive concrete strength was especially advantageous when the load eccentricity was small. When the eccentricity was increased, the strength of the high-strength concrete columns decreased more rapidly than that of the normal-strength columns. However, the high-strength concrete columns still exhibited a greater load capacity than the normal-strength columns.

INTRODUCTION

The introduction of high-strength concrete has made it possible to design columns more slenderly, and thereby facilitate not only new architectural ideas but also economic benefits. An increase in compressive strength allows smaller cross sections that require less concrete and permit more rentable floor space; however, although it can reduce column size, the columns become less ductile due to the brittleness of high-strength concrete.The performance of structural elements made of high-strength concrete has recently become a major concern for design engineers. Many aspects, such as ductility, amount of reinforcement, effect of slenderness, and eccentricity of the applied load, have to be investigated in order to understand the behavior of the columns completely. Some researchers, for example Ahmed and Shah (1982), Mander et al. (1988), Saatcioglu and Razvi (1992), and Cusson and Paultre (1994), have studied short columns of normal- and high-strength concrete subjected to axial loading. Only a few have studied full-scale reinforced high-strength concrete columns under eccentrically applied axial load: for example Bjerkeli et al. (1990), Lloyd and Rangan (1993), and Ibrahim and MacGregor (1996). However, the behavior of reinforced high-strength concrete columns is not yet fully understood. Often the results of these studies lead to empirical recommendations based on individually performed test series. In view of the economic limitations that prevent complete test series from being carried out, it would be of great benefit to establish a suitable numerical model that reflects the structural behavior accurately.

At the Division of Concrete Structures at Chalmers University of Technology, Göteborg, Sweden, a research program on reinforced columns made of high-strength concrete is being carried out, combining experiments and numerical simulations. In this study, 12 full-scale slender columns with square sections have been tested to failure under eccentric axial loading. The four parameters varied in this investigation were the concrete strength, stirrup spacing, slenderness, and eccentricity of the applied compressive load. In addition, the mechanical properties, such as the compressive and the tensile concrete and steel strengths, the modulus of elasticity and the fracture energy, were measured in the experimental investigation. These material properties were incorporated into a model in which the material model for concrete was based on nonlinear fracture mechanics. This model was, in turn, used in a nonlinear finite-element (FE) program in order to predict the responses of the slender concrete columns.

This paper describes the test program and the numerical aspect of the research program. The FE model used in the analysis is presented, followed by verification of the experimental results. Observations of the failure mechanisms during the tests and the results of the analysis, as well as some reasons for the failure of the columns under eccentric compressive loading, are presented. Some effects of slenderness that were investigated are reported.

TEST PROGRAM

Geometry and Configuration

The structural behavior of long, slender reinforced concrete columns subjected to eccentric axial loading is treated here.

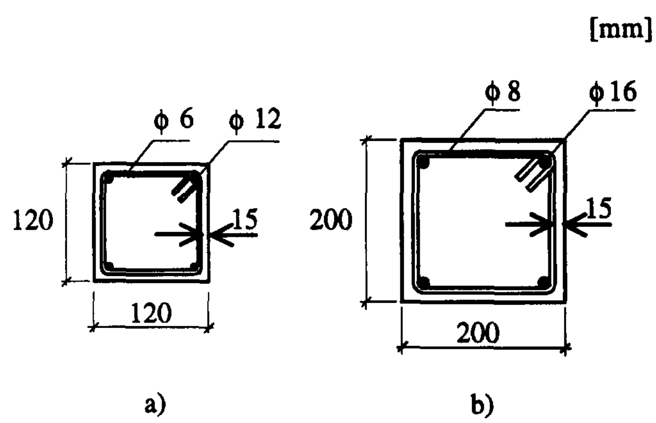

FIG. 1. Concrete Columns: Geometry and Details of Configurations (a) and (b)

TABLE 1. Details of Columns in Groups A, B, and C

Column group (1)	Length (mm) (2)	Configuration (3)	Eccentricity (mm) (4)	Stirrup spacing, s (mm) (5)	s/d_b (6)
A	2,400	a	20	100/180	8.3/15
B	3,000	b	20	130/240	8.1/15
C	4,000	b	20	130/240	8.1/15

[1]Grad. Student, Div. of Concrete Struct., Chalmers Univ. of Technol., S412 96 Göteborg, Sweden.

[2]Prof., Div. of Concrete Struct., Chalmers Univ. of Technol., S412 96 Göteborg, Sweden.

Note. Associate Editor: David J. Stevens. Discussion open until August 1, 1998. To extend the closing date one month, a written request must be filed with the ASCE Manager of Journals. The manuscript for this paper was submitted for review and possible publication on September 25, 1996. This paper is part of the *Journal of Structural Engineering*, Vol. 124, No. 3, March, 1998. ©ASCE, ISSN 0733-9445/98/0003-0233–0240/$4.00 + $.50 per page. Paper No. 14209.

TABLE 2. Composition of Concrete Mixes

Composition (1)	Normal-Strength Concrete A(I) (kg/m³) (2)	B(I) (kg/m³) (3)	C(I) (kg/m³) (4)	C(II) (kg/m³) (5)	High-Strength Concrete A(I) (kg/m³) (6)	B(I) (kg/m³) (7)	B(II) (kg/m³) (8)	C(I) (kg/m³) (9)	C(II) (kg/m³) (10)
Water	179	189	219	221	163	156	156	176	172
Portland cement	344	370	340	340	585	500	500	556	556
Silica fume	—	—	—	—	110	50	50	100	100
Sand	1,000	980	997	997	1,000	799	799	893	893
Crushed stone (gneiss) 8/12	—	—	—	—	485	954	954	622	622
Crushed stone (gneiss) 8/16	—	870	—	—	—	—	—	—	—
Crushed stone (gneiss) 8/24	794	—	853	853	—	—	—	—	—
Superplasticizer	—	—	—	—	17	13	11	14	14
Density (28 days)	2,370	2,370	2,340	2,339	2,362	2,525	2,520	2,428	2,411

TABLE 3. Properties of Hardened Concrete at 28 Days (Mean Strength of Three Specimens)

Specimen[a] (1)	$f_{c,cube}$ (MPa) (2)	$f_{c,cyl}$ (MPa) (3)	$f_{t,split}$ (MPa) (4)	E_0 (GPa) (5)	E_c (GPa) (6)
N-A(I)	58	43	4.2	—	—
H-A(I)	106	86	5.6	—	—
N-B(I)	43	33	3.7	26.0	25.0
H-B(I)	116	91	7.4	42.5	41.5
H-B(II)	112	92	7.4	41.0	40.0
N-C(I)	49	37	3.8	27.5	28.5
N-C(II)	49	37	3.7	27.5	29.0
H-C(II)	118	93	6.6	41.5	43.0
H-C(I)	119	93	6.2	41.0	42.5

[a]N = normal-strength; H = high-strength.

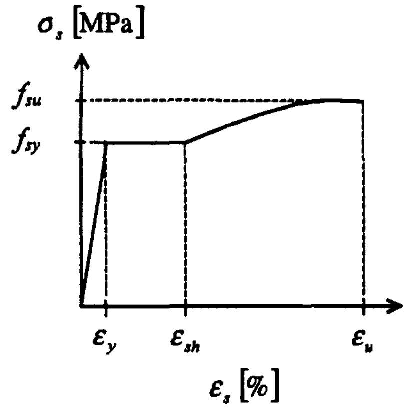

FIG. 2. Mechanical Properties of Reinforcement Bars

TABLE 4. Mechanical Properties of Reinforcement Bars

Specimen (1)	A_s (mm)² (2)	f_{sy} (MPa) (3)	f_{su} (MPa) (4)	ε_{sh} (%) (5)	ε_u (%) (6)	E_s (GPa) (7)
ϕ 16 Ks60	199	636	721	2.2	10	207
ϕ 12 Ks60	112	684	820	2.1	16	207
ϕ 8 Ks40S	50	466	620	4.0	12	221
ϕ 6 Ks40S	29	512	631	—	10	216

The test series consisted of 12 slender columns, with target compressive cube strengths of either 50 or 120 MPa. Half of the columns were made of normal-strength concrete, the other half of high-strength concrete. The lengths of the columns were 2.4, 3.0, or 4.0 m, with square cross sections as shown in Fig. 1. The thickness of the concrete cover, measured to the outer edge of the stirrup, was 15 mm for all of the columns. For each slender column, an identical short stub column was cast. The results of tests on these short stub columns have been reported in Claeson (1995). The parameters varied in the tests reported here were the concrete strength, the stirrup spacing, and the slenderness of the columns. Table 1 shows the different parameters of the test columns. The 2.4-m columns of group A were used in a pilot study. The larger stirrup spacings were chosen as the largest spacings allowed, $15d_b$, in the Swedish Code, BBK 94 (Boverket 1994).

Material Properties

The concrete mixes, designed with target compressive cube (150 mm) strengths of 50 and 120 MPa, were produced at the structural engineering laboratory at Chalmers University of Technology. Silica fume and plasticizer were used in the high-strength concrete mixes to obtain high strength, workability, and reduction of fine particle segregation. The detailed concrete composition is presented in Table 2. The properties of hardened concrete at 28 days are given in Table 3. The compressive cylinder strength, $f_{c,cyl}$, and the compressive cube strength, $f_{c,cube}$, refer to compression tests on specimens of sizes $\phi150 \times 300$ mm and $150 \times 150 \times 150$ mm, respectively. The splitting strength $f_{t,split}$, refers to tests on specimens $150 \times 150 \times 150$ mm and is approximately 90% of the flexural tensile strength ("CEB-FIP Model Code 1990" 1993). Here E_0 is measured in accordance with the definition in "CEB-FIP Model Code 1990" (1993); and E_c, in accordance with ISO norms. The elasticity of modulus was not measured for column group A. Due to the size of the concrete mixer, two batches each had to be made for the normal- and high-strength concrete in group C, and for the high-strength concrete in group B. For the remaining mixes, the amount of concrete needed could be made in one batch, with the exception of the normal-strength concrete of group B, which was fabricated and delivered by a local producer. The column specimens were cast horizontally in steel forms. The concrete was thoroughly vibrated by means of an internal vibrator. Very little bleeding was observed. The columns were demolded after approximately seven days and cured under laboratory conditions until tested.

Deformed bars of Swedish type Ks40S were used as the lateral reinforcement and Ks60 for the longitudinal reinforcement. The mechanical properties of the steel reinforcement are presented in Fig. 2 and Table 4. All of the stirrups were anchored with 135° bends extending approximately 70 min into the confined concrete core.

Test Setup

The slender columns were hinged at the ends and the load was applied with an initial eccentricity of 20 mm at both ends. The hinge was formed by a curved bearing plate of steel that was fixed to a thick steel plate in contact with the column end (Fig. 3). The position of the column on the steel plate was adjusted by means of alignment bolts placed in angle bars.

The buckling length of the simply supported column is the distance between the bearings at each support.

All of the tests were carried out in a Losenhausen vertical hydraulic column testing machine with a capacity of 10,000 kN. The load, which was determined by measurements from an oil pressure gauge, calibrated against the testing machine prior to the column tests, was increased at a constant rate without interruption. The actuators have hydrostatic bearings, which implies negligible friction. When the load approached the calculated maximum load, the oil pressure gauge was used to indicate how the deformation should be increased in order to capture the postpeak curve.

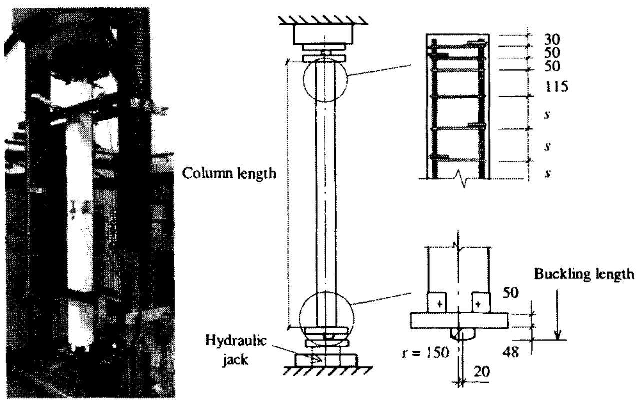

FIG. 3. Load Arrangement for Slender Columns (Dimensions in Millimeters)

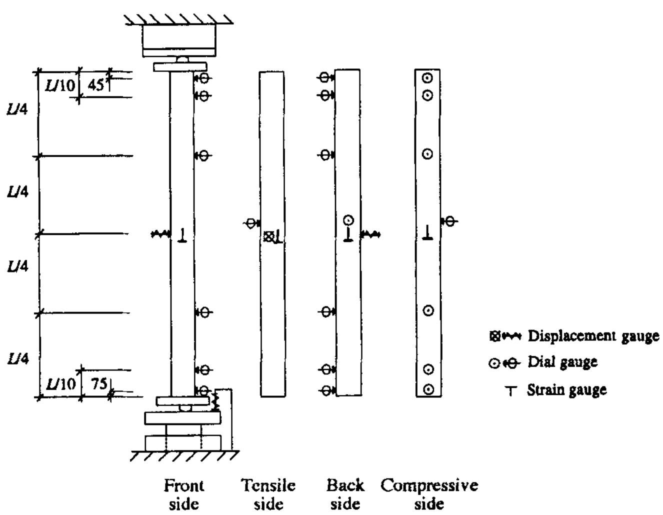

FIG. 4. Instrumentation of Slender Columns

The deflection in the bending direction was measured at seven locations in order to determine the deflected shape of the column (Fig. 4). Another dial gauge was used to check for possible biaxial bending in the perpendicular direction. The vertical displacement of the lower movable plate of the column testing machine was measured in relation to the laboratory floor by a displacement transducer. For each specimen, a vertical and a horizontal 60-mm-long strain gauge were glued to the concrete at each side of the column at midheight, 6-mm-long strain gauges were glued onto each of the longitudinal reinforcement bars at midheight, and 3-mm-long strain gauges were glued onto the stirrups on each side at midheight. To ensure that the failure would occur in the instrumented region of the columns, the ends of the test specimens were further confined with stirrups spaced apart 50 mm or less (Fig. 3).

The top cast side is the weakest of the sides; it was decided to position this side in the test machine so as to be the compressive side in the tests. This would give us a lower boundary value of bearing capacity.

TEST RESULTS

The columns were all tested after approximately 28 days. The duration of each test was 1 1/2–2 hours, which corresponds to a loading rate of 10–20 kN/min. Table 5 presents the results of the tests. The length-to-width ratio, defined as the ratio of the column length, L, to the cross-section dimension, h, was either 15 or 20.

The ascending branches of the high-strength concrete columns were almost linear. No spalling of concrete cover and very few tensile cracks before reaching the maximum load were observed. The high-strength concrete columns exhibited a rather sudden and explosive type of failure, especially the columns with a length-to-width ratio of 15. It appears that the capacity of the compressed concrete determined the maximum load. The sudden failure may also be due to the fact that the load was applied in a load-controlled manner. Although the test machine has a closed-loop system, it may not react quickly enough to secure a steady postpeak curve for the high-strength concrete columns. The behavior of the high-strength concrete columns differed from that of the normal-strength concrete columns, which exhibited major softening on the compressive side including spalling of parts of the concrete cover before reaching the maximum load. Furthermore, the normal-strength columns displayed more tensile cracks. The column failure location varied from midheight to an extreme of 500 mm below midheight. A characteristic feature of the failure surface was that the tension face exhibited a horizontal bending crack or cracks across the width of the column. On the compressed side, a concrete section, the width of the side and approxi-

TABLE 5. Results from Tests on Slender Columns

Column number (1)	Column group and batch (2)	Concrete strength (3)	$f_{c,cyl}$ (MPa) (4)	$f_{c,cube}$ (MPa) (5)	Longitudinal reinforcement ratio (%) (6)	Stirrup spacing (mm) (7)	Maximum load (kN) (8)	Midheight deflection (mm) (9)	Maximal FE-load (kN) (10)	Midheight FE-deflection (mm) (11)
23	A (I)	Normal	43	58	3.2	100	320	26	288	19
24	A (I)	Normal	43	58	3.2	180	280	24	288	19
25	A (I)	High	86	106	3.2	100	370	36	380	25
26	A (I)	High	86	106	3.2	180	330	47	380	25
27	B (I)	Normal	33	43	2.1	130	990	22	1,033	25
28	B (I)	Normal	33	43	2.1	240	990	21	1,033	25
29	B (I)	High	91	116	2.1	130	2,310	23	2,364	22
30	B (II)	High	92	112	2.1	240	2,350	20	2,364	22
31	C (II)	High	37	49	2.1	130	900	40	866	35
32	C (II)	Normal	37	49	2.1	240	920	36	866	35
33	C (II)	High	93	118	2.1	130	1,530	39	1,535	33
34	C (I)	High	93	119	2.1	240	1,560	41	1,535	33

mately 2.5 times this in length, fell off the high-strength concrete columns at maximum load. The loss of the protecting cover combined with a high load level finally led to buckling of the vertical reinforcement bars at the end of the test (Fig. 5). The tests were terminated when midheight deflection was approximately 5% of the column length. Beyond this value of deflection, an instability failure of the whole column was feared.

All columns failed due to crushing of the concrete cover. Of the reinforcement bars in the columns of all three groups, none had reached yielding at maximum load. However, in both the high-strength and normal-strength concrete columns, the bars with spacing of 130 mm were close to yielding at maximum load. The strains in the bars of the column with stirrup spacing of 130 mm were greater than the strains in the bars of the column with 240-mm stirrup spacing. It was observed during the tests that while the closer stirrup spacing did not increase the load capacity, it did give the column a less brittle failure. This was the case for both the normal- and high-strength concrete columns with the larger cross section. The testing of column group A was conducted as a pilot study with a larger cover-to-core ratio than the columns of groups B and C; accordingly, the results of these tests could be slightly misleading when comparing the different groups.

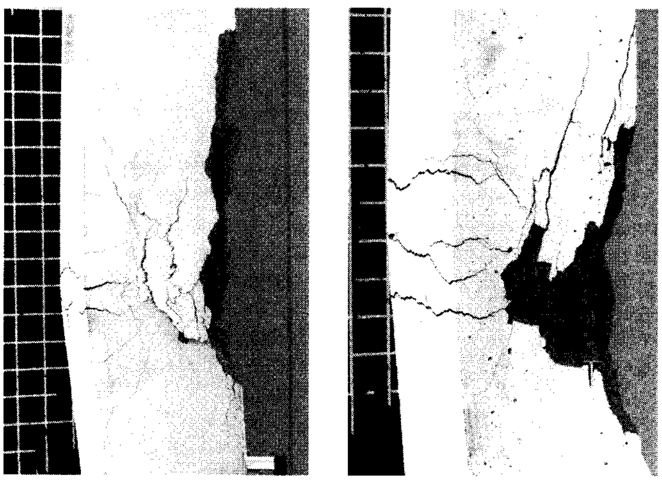

a) b)

FIG. 5. Final Failure of Specimens: (a) #27 (3.0 m Normal-Strength Concrete); and (b) #29 (3.0 m High-Strength Concrete); Photos Were Taken after Completion of Tests

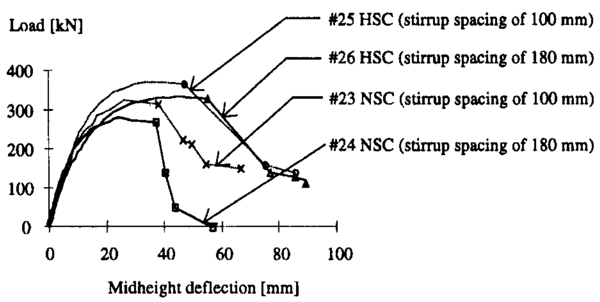

FIG. 6. Measured Load versus Midheight Deflection of 2.4 m Slender Columns in Group A

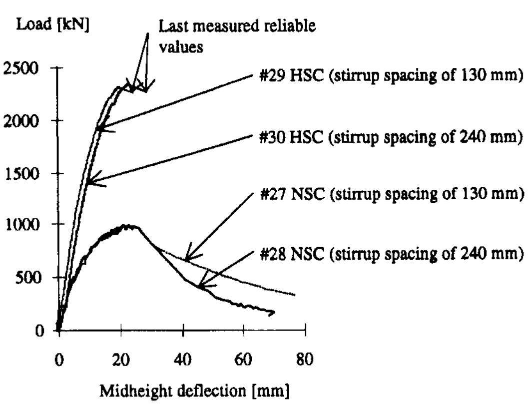

FIG. 7. Measured Load versus Midheight Deflection of 3.0 m Slender Columns in Group B

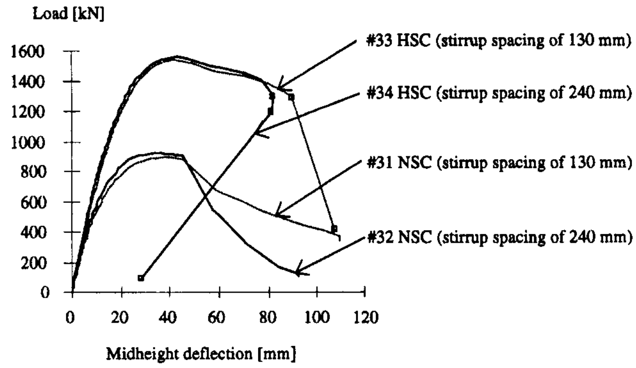

FIG. 8. Measured Load versus Midheight Deflection of 4.0 m Slender Columns in Group C

In Figs 6 – 8, the measured load versus midheight deflection relations are compared for the three different groups of columns. In Figs. 6 and 7, markers have been included on the descending load branches to indicate the actual measured values. As can be observed from the figures and Table 5, the midheight deflection is approximately the same at the measured maximum load for the same cross section, length-to-width ratio, and initial load eccentricity. Design calculations of deflection curves for pinned columns often assume a sine-shaped deflection. While this assumption may yield fairly good predictions of the failure load and the ascending portion of the load-deflection curve, it is probably too approximate to predict the postpeak behavior of test columns as also observed by Lloyd and Rangan (1996). This observation is one reason why a nonlinear sectional analysis of the critical segment combined with a simplified approach for capturing the second-order deflections has not been used in the following analysis.

FINITE-ELEMENT ANALYSIS

General

One of the aims of the study was to develop nonlinear FE models that could simulate the failure mechanism of the columns and, together with the experiments, made possible a better understanding of the mechanical behavior until final failure, including the postpeak behavior. These models were generated in the nonlinear FE program ABAQUS (*ABAQUS* 1995). A model based on three-dimensional three-node hybrid beam elements was established. The advantage of a beam element model is that it can be run in a reasonable amount of time. However, the amount of information obtained is more limited than with a solid element model. Nevertheless, the beam element model was chosen for this study, as it was believed to give the required information. Furthermore, a previous study had shown good agreement between the results of an analysis using beam elements and one using solid elements (Claeson 1995). Approximately 50 elements were used for all lengths. The model included the four vertical reinforcement bars; however, the stirrups could not be modeled. The reason this was not considered to be a major disadvantage is that the main effect of the stirrups, with a spacing of 130 or 240 mm, in columns subjected to eccentric loading is to prevent the reinforcement bars from buckling and not, as in the centric compressive case, to produce a triaxial stress state. In the model the reinforcement bars cannot buckle; in other words, the model simulates a column where this is not a problem. Although this somewhat limits the study, the model does simulate the structural behavior accurately up to maximum load, as well as to the point when the reinforcement bars would buckle in reality. For columns tested with an initial eccentricity of 20 mm, this happened at a very late stage in the normal-strength concrete columns. However, the behavior of the high-strength concrete columns may be looked upon as a model simulating a column with close stirrup spacing. As the eccentricity increases, the tendency of the reinforcement bars to buckle decreases; also, any buckling that occurs is at a later stage of the postpeak curve. This conclusion was also reached by Lloyd and Rangan (1996), who stated that no buckling of the reinforcement bars in their tests was observed.

To model reinforced concrete, the program ABAQUS combines standard elements of plain concrete with a special option, called rebar. This option strengthens the concrete in the direction chosen, thereby simulating the behavior of a reinforcement bar. By this approach, the material behavior of the plain concrete is taken into account independently of the reinforcement.

Constitutive Models for Concrete and Reinforcement

The material model for concrete provided in ABAQUS was used in the analysis. When the principal stress components are compressive, the response of the concrete is modeled by an elastic-plastic model. The uniaxial compressive stress-strain relations used in the FE analysis were based on cylinder tests. These cylinders ($\phi 150 \times 300$ mm), cast with concrete from the same batch as the columns, were used to test the modulus of elasticity. The compressive strengths obtained from these tests were slightly higher than the values received from the pure compressive cylinder tests. However, from the pure compressive cylinder tests only the maximum compressive strengths were obtained; there was no measured ascending branch. Therefore, the ascending branch and the compressive values from the modulus of elasticity tests were used. The relations between the compressive stress and the plastic strain are shown in Fig. 9. The descending branches chosen were based on relevant data found in the literature (Cusson and Paultre 1994).

The smeared crack approach has been chosen to model cracked reinforced concrete. According to the smeared crack concept, a cracked solid is imagined to be a continuum for stress and strain. This means that the behavior of cracked concrete can be described in terms of stress-strain relations. Prior to cracking, the concrete is modeled sufficiently accurately in tension as an isotropic, linear elastic material. The fracture energy was determined from tests on three-point bending beams (RILEM 50-FMC Committee 1985) and, together with the tensile strength and the crack spacing from the tests, was used to calculate the tensile softening relation [Fig. 9(b)].

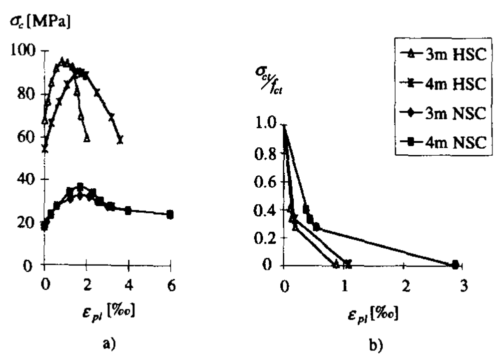

FIG. 9. Uniaxial Stress-Strain Relations Used in Finite-Element Analysis: (a) Compressive Stress versus Plastic Strain; (b) Tensile Stress Ratio versus Plastic Strain

The longitudinal reinforcement bars were modeled by a linear elastic-plastic material model. The modulus of elasticity, the yield strength, and the ultimate strength of the reinforcement bars were determined through tension tests (Fig. 2; Table 4), and the Poisson ratio was approximated to be 0.3.

Results of Finite-Element Analysis

A comparison of the load deflection curves from tests and the analysis shows that the FE beam model does capture the structural behavior of the columns satisfactorily (Fig. 10). The load-deflection curves of the columns subjected to an initial eccentricity of 20 mm were compared with the results of the tests to validate the accuracy of the model. In all of the cases analyzed, the accuracy was found to be satisfactory. It follows from Table 5 that the maximum loads obtained from the FE analysis are equal to the test strengths to within 10%. However, it was observed that the results from the FE analysis gave

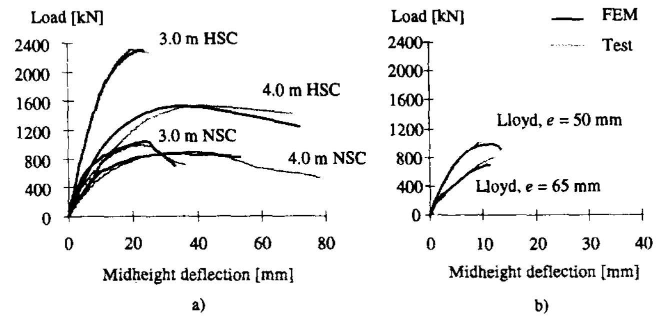

FIG. 10. Comparison of Results of Finite-Element Analysis (Dark Line) and Tests (Light Line) by: (a) Claeson (1995); (b) Lloyd and Rangan (1993)

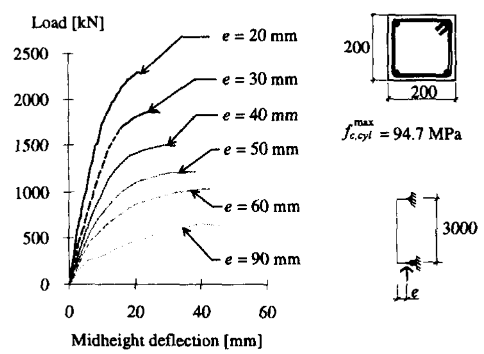

FIG. 11. Load versus Midheight Deflection Relation for 3.0 m High-Strength Concrete Column Subjected to Different Initial Load Eccentricities

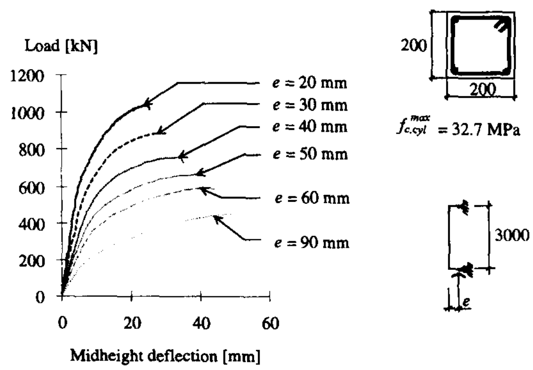

FIG. 12. Load versus Midheight Deflection Relation for 3.0 m Normal-Strength Concrete Column Subjected to Different Initial Load Eccentricities

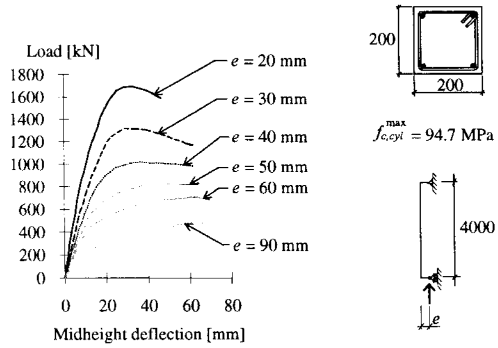

FIG. 13. Load versus Midheight Deflection Relation for 4.0 m High-Strength Concrete Column Subjected to Different Initial Load Eccentricities

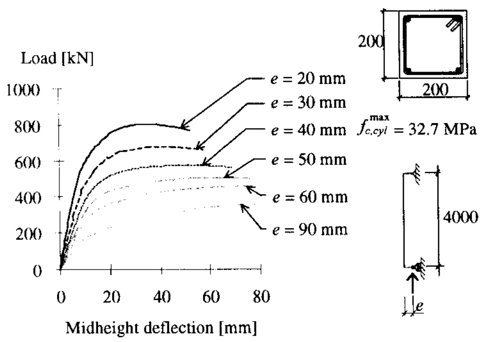

FIG. 14. Load versus Midheight Deflection Relation for 4.0 m Normal-Strength Concrete Column Subjected to Different Initial Load Eccentricities

a stiffer initial behavior than that of the tests. This discrepancy is primarily attributed to the formulation of the beam element and the differences between the measured and modeled geometric and material imperfections. To validate the model for larger eccentricities, two high-strength concrete columns tested by Lloyd and Rangan (1993) were analyzed. The columns had a length of 1.6 m and a quadratic cross section with 175-mm sides. The two columns chosen were subjected to eccentricities of 50 and 65 mm. The results of the tests and the analysis of these columns are included in Fig. 10. The FE analysis was terminated in all cases owing to numerical problems.

To enable a comparative study of the influence of different eccentricities on structural behavior, for the two different length-to-width ratios and concrete strengths, one high-strength concrete and one normal-strength concrete were chosen (the 3.0 m values). Figs. 11 – 14 show the results of the simulations of columns subjected to different initial load eccentricities.

ANALYSIS

The columns of group A had a thicker concrete cover in relation to the cross section, as well as a smaller cross section, than the rest of the columns. It was noted during the tests that although the cracks appeared early, contrary to the observations of other researchers, the same cracks continued to grow and no others appeared until very close to the peak load. Apparently, small cross sections in high-strength concrete are very sensitive to both the curing conditions and the amount of vibration.

The tests show clearly that the minimum stirrup spacing, $15d_b$, required by BBK 94 (Boverket 1994), is not sufficient to secure a ductile failure for small load eccentricities in high-strength concretes. To obtain a ductile failure, very close stirrup spacing or maybe even a steel cover, as in composite columns, is necessary. However, as this is not always an economical solution, a new design philosophy may be needed.

The length-to-width ratio, defined as the ratio of the column length, L, to the cross-section dimension, h, was either 15 or 20. The structural behaviors of these two length-to-width ratios with configuration (b) (Fig. 1), subjected to different eccentricities were studied. The high-strength concrete columns with a length-to-width ratio of 20 exhibited a less brittle behavior than the high-strength concrete columns with a length-to-width ratio of 15 (Figs. 11 – 14); the deflection was greater and the maximum load capacity less. The same observations apply to the normal strength columns. From the results of the FE analysis, it was observed that the midheight deflection for the columns with a length-to-width ratio of 15 was almost the same for the same initial eccentricity regardless of the concrete strength. It was when the eccentricity was 90 mm that the deflection of the two strengths started to differ. For a length-to-width ratio of 20, the midheight deflection was approximately the same for the two types of concrete when the eccentricity was 20 mm. This was also observed by Lahoud (1991). However, for the other eccentricities, the high-strength concrete columns had a midheight deflection that was approximately 10 mm less than the deflection of the normal-strength concrete columns. The same midheight deflection of the columns subjected to small eccentricities may be explained by the fact that the two types of concrete have almost the same deformation capacity, i.e., the maximum load divided by the secant modulus for high-strength concrete columns is approximately the same as that of the normal-strength concrete columns.

Fig. 15 presents the influence of eccentricity, e, on the maximum strength of columns for length-to-width ratios, L/h, of 15 and 20; P_{max} denotes the maximum load capacity of the columns. It is clear that column capacity is strongly affected by the amount of eccentricity. However, although the same trend is observed for both normal- and high-strength concrete columns as e increases, the strength of the high-strength concrete columns decreases more rapidly than that of the normal-strength concrete columns. The ratio of the maximum capacities of the high-strength concrete columns with length-to-width ratios of 15 and 20 was 1.5 when the eccentricity was 20 mm but decreased as the eccentricity increased. When the eccentricity was 90 mm, this ratio had decreased to 1.4. In contrast, the ratio remained almost constant at 1.3 for the normal-strength concrete columns (Fig. 15).

Fig. 15 also illustrates the different failure modes. The fail-

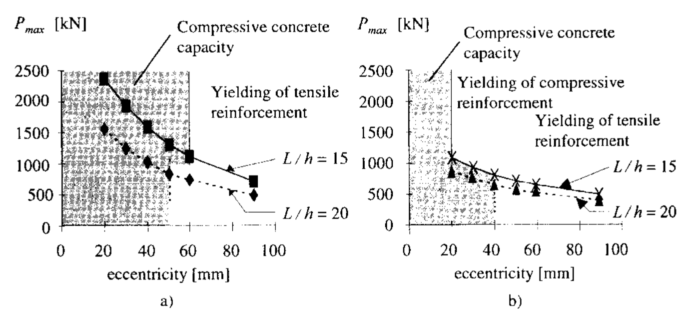

FIG. 15. Effect of Eccentricity on Maximum Load of Different Slenderness Ratios and Concrete Strengths: (a) High-Strength Concrete; (b) Normal-Strength Concrete

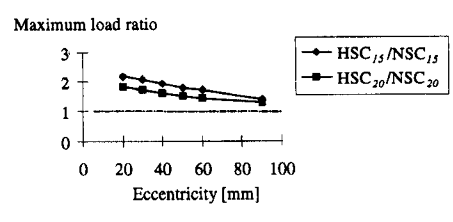

FIG. 16. Maximum Load Ratio versus Eccentricity for Two Slenderness Ratios and Concrete Strengths

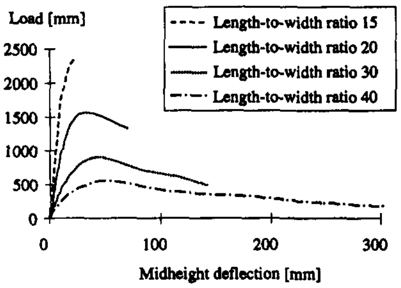

FIG. 17. Effect of Slenderness on High-Strength Concrete Columns Subjected to Initial Eccentricity of 20 mm

ure modes differed with varying eccentricity. When the eccentricity was small, the shape of the compression curve and the maximum compressive strength were the determining factors. However, when the eccentricity increased, the yielding of the reinforcement bars determined the maximum load. This trend was the same for both length-to-width ratios and concrete strengths, although the behavior was more prominent for the columns with a length-to-width ratio of 20.

The maximum load ratio is the ratio between the maximum load of the high-strength concrete columns and that of the normal-strength concrete columns. Fig. 16 shows that when the concrete strength is increased, the load capacity increases. This was the case for all of the eccentricities in this study. The advantage of using high-strength concrete is the greatest when the eccentricity is small. However, gains in strength are achieved even when the eccentricity is quite large.

To study the slenderness effect, two additional length-to-width ratios were added: 30 and 40. Although these length-to-width ratios have not been verified by testing, they are included in this study to demonstrate the capacity of the FE model. The columns with length-to-width ratios of 30 and 40 failed due to instability. Fig. 17 shows the relation between the load and the midheight deflection for four high-strength concrete columns subjected to an initial eccentricity of 20 mm. When the length-to-width ratio increases, the load-bearing capacity and the advantage of using a higher compressive concrete strength decrease.

CONCLUSIONS

The results of tests and the FE analysis on slender, square reinforced concrete columns presented here allow the following conclusions to be drawn. The failures of the high-strength concrete columns were brittle. While the closer stirrup spacing did not increase the load capacity, it did contribute to a less brittle behavior after the maximum load had been reached. However, it was observed from the tests of high-strength concrete columns that a closer stirrup spacing is required to obtain the same structural behavior as that of the normal-strength concrete columns.

Four failure modes were observed. When the load eccentricity was small, the compressive strength of concrete played a dominant role; when the eccentricity was increased, yielding of the compressive reinforcement bars determined the maximum load; and when the eccentricity was large, the yielding of the tensile reinforcement bars determined the maximum load. This was the case for both the high- and the normal-strength concrete columns with a length-to-width ratio of 15 or 20. However, the first failure mode dominated for the high-strength concrete columns, while the two other modes did so for the normal-strength concrete columns. The high-strength concrete columns with a length-to-width ratio of 30 or 40 failed due to instability.

The midheight deflections at maximum load for a length-to-width ratio of 15, with the same initial load eccentricities and cross sections, were almost the same regardless of concrete strength. For a length-to-width ratio of 20, the deflections of the normal-strength concrete columns were slightly greater than the deflections of the high-strength concrete columns.

The influence of eccentricity on column strength for two different length-to-width ratios and concrete strengths was studied. The column strength is strongly affected by the amount of the eccentricity. Although the same trend is observed for both normal- and high-strength concrete columns, it was found that when the eccentricity increased, the strength of the high-strength concrete columns decreased more rapidly than that of the normal-strength columns. In addition, the high-strength concrete columns with a length-to-width ratio of 15 obtained higher load capacities than either those with a length-to-width ratio of 20 or the normal-strength concrete columns with length-to-width ratios 15 and 20.

ACKNOWLEDGMENTS

This project is a part of a national research project that treats the properties of high-strength concrete. The writers appreciate the financial support of the Swedish Building Council, Nutek, and the building companies Strängbetong, NCC, Skanska, Cementa, Elkem Materials, and Euroc Beton.

APPENDIX I. REFERENCES

ABAQUS theory manual, version 5.5. (1995). Hibbit, Karlsson & Sorensen Inc., Providence, R. I.

Ahmed, S. H., and Shah, S. P. (1982). "Stress-strain curves of concrete confined by spiral reinforcement." *ACI J., Proc.*, 79(6), 484–490.

Bjerkeli, L., Tomaszewics, A., and Jensen, J. J. (1990). "Deformation properties and ductility of high strength concrete." *Utilization of High-Strength Concrete—2nd Int. Symp., SP-121*, American Concrete Institute, Detroit, Mich., 215–238.

Boverket. (1994). "Boverkets handbok för betongkonstruktioner [manual for concrete structures from the Swedish Board of Housing, Building and Planning]." *BBK 94, Band 1, Konstruktion*, Byggavdelningen, Karlskrona, Sweden (in Swedish).

"CEB-FIP Model Code 1990." (1993). *CEB Bull. d'Information No. 213/214.* Comité Euro-International du Béton, Lausanne, Switzerland.

Claeson, C. (1995). "Behavior of reinforced high strength concrete columns," Licentiate thesis, Publication 95:1, Division of Concrete Structures, Chalmers University of Technology, Göteborg, Sweden.

Cusson, D., and Paultre, P. (1994). "High-strength concrete columns confined by rectangular ties." *J. Struct. Engrg.*, ASCE, 120(3), 783–804.

Ibrahim, H. H. H., and MacGregor, J. G. (1996). "Tests of eccentrically loaded high-strength concrete columns." *ACI Struct. J.*, 93(5), 585–594.

Lahoud, A. E. (1991). "Slenderness effects in high-strength concrete columns." *Can. J. Civ. Engrg.*, 18, 765–771.

Lloyd, N. A., and Rangan, B. V. (1993). "High-strength concrete columns under axial load and uniaxial bending." *Utilization of High-Strength Concrete—3rd Int. Symp. Proc.*, 2, Norwegian Concrete Association, Oslo, Norway, 1217–1224.

Lloyd, N. A., and Rangan, B. V. (1996). "Studies on high-strength concrete columns under eccentric compression." *ACI Struct. J.*, 93(6), 631–638.

Mander, J. B., Priestley, J. N., and Park, R. (1988). "Observed stress-strain behavior of confined concrete." *J. Struct. Engrg.*, ASCE, 114(8), 1827–1849.

RILEM 50-FMC Committee. (1985). "Determination of the fracture energy of mortar and concrete by means of three-point bend tests on notched beams." *Mat. and Struct.*, Paris, France, 18, 285–290.

Saatcioglu, M., and Razvi, S. R. (1992). "Strength and ductility of confined concrete." *J. Struct. Engrg.*, ASCE, 118(6), 1590–1607.

APPENDIX II. NOTATION

The following symbols are used in this paper:

A_s = area of reinforcement bar;
d_b = diameter of longitudinal reinforcement bar;
E_0 = modulus of elasticity for concrete defined in CEB-FIP Model Code 1990;
E_c = modulus of elasticity for concrete in accordance with ISO norms;

E_s = modulus of elasticity of steel reinforcement;
e = eccentricity;
$f_{c,cube}$ = compressive cube (150 × 150 × 150 mm) strength of concrete;
$f_{c,cyl}$ = the compressive cylinder (ϕ150 × 300 mm) strength of concrete;
$f_{c,cyl}^{max}$ = the compressive cylinder strength of concrete from E-modulus tests;
f_{ct} = maximum tensile concrete strength;
f_{su} = ultimate strength of reinforcement bar;
f_{sy} = yielding strength of reinforcement bar;
$f_{t,split}$ = splitting cube (150 × 150 × 150 mm) strength of concrete;
h = width of cross section;
L = length of column;
L/h = length-to-width ratio;
N = axial load;
P_{max} = maximum load bearing capacity of the column;
r = radius of load bearing;
s = stirrup spacing;
ε_{pl} = plastic strain in concrete;
ε_s = steel strain;
ε_{sh} = strain when hardening of reinforcement bar starts;
ε_u = ultimate strain of reinforcement bar;
σ_c = concrete compressive stress; and
ϕ = diameter.